Study of the Advence Virgo timing resolution for the inspiral low latency pipeline MBTA with software injections

Michael V. Bebronne

Laboratoire d'Annecy-le-Vieux de Physique des Particules

9 Chemin de Bellevue

BP 110, 74941 Annecy-le-Vieux, France

June 6, 2012

Introduction

The purpose of this note is to summarize results concerning the timing resolution of the low latency inspiral pipeline MBTA (see [1, 2] for descriptions of MBTA) obtained with runs of software injections. These software injections were made in a virtual interferometer with Advance Virgo (AdV) like spectrum (see Fig. 1). They were motivated by tho main questions:

- What timing resolution is to be expected from an advance detector configuration?
- There always was a discrepancy between the theoretical timing resolution and the observed one. Could we understand the origin of this discrepancy? Is there something which can be done to reduce it?

The timing accuracy of an inspiral search pipeline strongly limit our ability to localize a source of gravitational wave, since localization occurs through triangulation with a network of detectors [2]. Hence, it is important to try to give an answer to those questions.

This note is organized as follows. First, we introduce the theoretical formulas used to determine the timing accuracy of a gravitational wave interferometer, and we will see what these formulas imply for different AdV sensitivity curves (Fig. 1). Then, we briefly discuss the timing resolution of the Virgo detector during the joined S6/VSR3 run. We carry on with some details about the runs of software injections: type of injections, method to create the signal, etc. Finally, we discuss our results.

Timing resolution

The theoretical timing resolution of a gravitational wave interferometer is given by the following formula [4]

$$dt = \frac{1}{2\pi\rho\sigma_f},$$

where ρ is the signal to noise ratio (SNR) and σ_f is the effective bandwidth given by

$$\sigma_f^2 = \bar{f^2} - \bar{f}^2 \quad \text{with} \quad \bar{f^n} \equiv 4\int_0^\infty \mathrm{d}f \frac{|\tilde{h}(f)|^2}{S(f)} f^n.$$

In these formulas, $S(f)$ is the noise power spectrum of the detector and the signal h is normalized such that

$$\langle h|h\rangle \equiv 4\mathrm{Re}\int_0^\infty \mathrm{d}f \frac{|\tilde{h}(f)|^2}{S(f)} = 1.$$

As an example, let us consider a binary neutron star (BNS) of equally mass (1.4-1.4 $\mathrm{M}_\odot$) located at an effective distance of 274.57 Mpc. Let us also make the approximation $\tilde{h}(f) \sim f^{-7/6}$ [5]. The following table resumes the theoretical SNR and timing accuracy of the Virgo detector for the five sensitivity curves describe in Fig. 1.

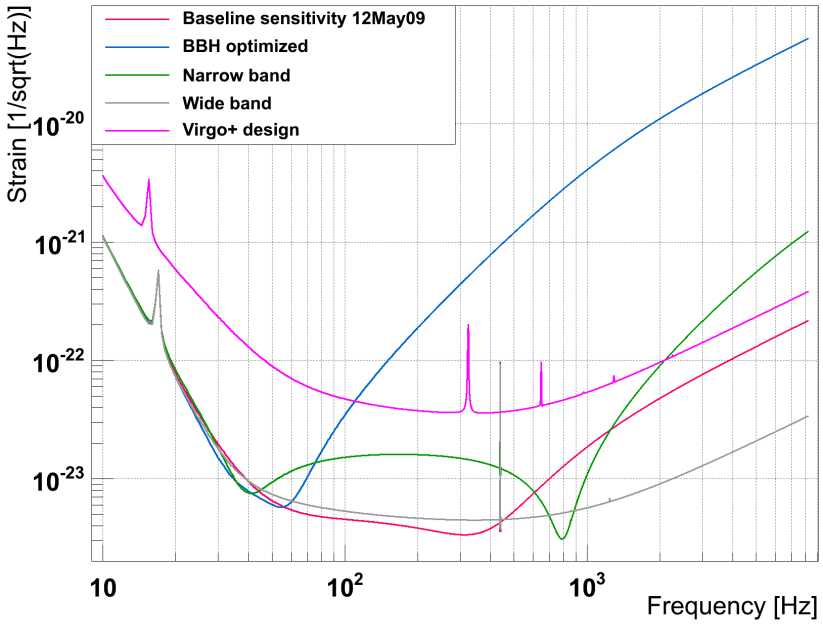

Figure 1: This plot shows different possible AdV sensitivity curves [3]. The red curve is the reference baseline sensitivity which maximizes the inspiral range for binary neutron stars (BNS). The blue curve is optimized for the detection of binary black holes (BBH) of 10 $M_{\odot}$. The green curve shows a narrow band tuning useful to target a monochromatic source. The grey curve, known as the wide band sensitivity, is designed to improve the high frequency sensitivity. Finally, the pink curve is the Virgo+ design sensitivity curve.

Sensitivity curve	**SNR**	**Range [Mpc]**	**dt [ms]**	**dt [ms] for fixed SNR = 10**
Baseline	10	153	0.16	0.16
BBH optimized	6.57	100	1.88	1.34
Narrow band	5.77	88	0.17	0.10
Wide band	8.76	134	0.12	0.11
Virgo+	0.9	14	1.15	0.10

As shown by this table, the theoretical timing resolution of AdV for BNS detection may vary between 0.12 ms for a wide band configuration up to 15 time more for a binary black holes (BBH) optimized spectrum.

Timing resolution of Virgo detector for the joined S6/VSR3 run

Up to now, there always was a discrepancy between the timing resolution really observed during a run and the predicted one. To illustrate this, let-us consider a few days of the S6/VSR3 run during which there were several hardware injections (between gps time 966800000 and 967800000). For this note, we have re-analyzed the data of the Virgo detector for that period with three different family of templates: GeneratePPNtwoPN, EOBNRpseudoFourPN and TaylorT4threePointFivePN templates. The following table summarizes our results (plots with more details are given in the appendix)

Templates	**dt [ms] (RMS)**	**dt [ms] (predicted)**	**Ref. Freq. [Hz]**	**Plot**
GeneratePPNtwoPN	0.28	0.08	150	Fig. 5
EOBNRpseudoFourPN	1.33	0.08	150	Fig. 6
TaylorT4threePointFivePN	1.267	0.08	150	Fig. 7

This table shows that there is a discrepancy between the real timing resolution and the one which is expected, and the size of this discrepancy seems to depend on the family of templates used for the matched-filtering. Now, two remarks are in order.

- First, the predicted timing resolutions are calculated with the observed SNR (and not with the predicted SNR). This is done to exclude the error coming from the discrepancy between the predicted and observed SNR.
- Second, all found injections were of the GeneratePPNtwoPN type, with the exception of one EOBNRpseudoFourPN injection (65 found injections for the GeneratePPNtwoPN and TaylorT4threePointFivePN analysis, 66 for the EOBNRpseudoFourPN one). Therefore, it is not surprising that the best results were obtained with the GeneratePPNtwoPN templates.

As stated in the introduction, trying to understand this discrepancy is one of the two main motivations to the runs of software injections described in this note.

Software injections

The runs of software injections discussed in this note were made of 200 compact binary coalescence (cbc) signals injected in Gaussian noise in order to simulate the output $h(t)$ of a gravitational wave interferometer. This simulated output is obtained by a three step process:

- creation of a list of 200 different simulated cbc with the *lalapps_inspinj* program available in LALsuite [6];
- generation of the gravitational wave signal corresponding to these 200 simulated events with the *lalapps_coinj* program also available in LALsuite;
- creation of a simulated output signal $h(t)$ containing these 200 simulated events in random Gaussian noise with a program called *MbSoftInject* (version v0r51 of April 21, 2011 with small modifications).

This last step uses a sensitivity curve to create the background Gaussian noise in which the simulated events are injected. It is also in this last process that the simulated events are rescaled as to appear as an output of MBTA with an SNR of 10.

The formula used by *MbSoftInject* to determine the theoretical SNR and therefore the rescaling factor to be applied is

$$\rho = 8\left(2.3 \times \frac{\text{Range}}{\text{Distance}}\right) \times \frac{M_1 M_2 \left(2.8\right)^{1/3}}{\left(1.4\right)^2 \left(M_1 + M_1\right)^{1/3}}.$$

Since this formula is based on non-spinning binary neutron stars of 1.4-1.4 $M_\odot$, the applied rescaling factor is correct for low mass non-spinning binaries and becomes less and less correct for increasing mass and spin (in other words, the theoretical SNR of the injected signals is equal to 10 for non-spinning low mass systems and could significantly differ for systems with higher mass or systems with spin). This should be kept in mind when considering spinning and heavier binary systems.

Four different type of binary systems are considered in this note: binary neutron stars (BNS) with masses 1.4-1.41 $M_\odot$, neutron star black hole (NSBH) with masses 1.4-7.8 $M_\odot$, binary black holes (BBH) of masses 7.8-7.81 $M_\odot$ and massive binary black holes (MBBH) of masses 30-30.1 $M_\odot$.

Finally, let us stress that, when different runs of injections where made with the same kind of binary system, the parameters of the 200 simulated events where kept the same. For example, when we will consider a run of 200 injected BNS generated with the *GeneratePPNtwoPN* model and a run of 200 injected BNS generated with the *EOBNRpseudoFourPN* model, the 200 simulated events have exactly the same parameters in both runs[1].

Results

The following tables (Fig. 2 and Fig. 3) resume the results and details of the different software injection runs which were made. Plots illustrating those results may be found in the appendix. The versions of MBTA used for this study were MbtaRT v0r59 for the first software injection runs (with GeneratePPNtwoPN templates) and MbtaRT v0r61 afterwards (which supports EOBNRpseudoFourPN and TaylorT4threePointFivePN templates).

[1]The only exception will concern injections with non-zero spin, which of course could not have the same parameters than non-spinning systems.

Sensitivity	Inspirial type	Injected Model	Research type	Templates	Ref. freq. [Hz]	SNR (Mean)	dt [ms] (RMS)	dt [ms] (gaussian fit)	dt [ms] (theory)	Distance (Mean in %)	Plot
Baseline	BNS	GeneratePPNtwoPN	Monotemplate	GeneratePPNtwoPN	-	9.85	0.24	0.20	0.16	101.9	Fig. 8
BBH opt.	BNS	GeneratePPNtwoPN	Monotemplate	GeneratePPNtwoPN	-	9.97	1.90	1.90	1.36	101.8	Fig. 9
Narrow band	BNS	GeneratePPNtwoPN	Monotemplate	GeneratePPNtwoPN	-	9.22	0.95	0.22	0.10	102.5	Fig. 10
Wide band	BNS	GeneratePPNtwoPN	Monotemplate	GeneratePPNtwoPN	-	9.93	0.21	0.14	0.10	102.4	Fig. 11
Baseline	BNS	GeneratePPNtwoPN	Grid 1.2-1.6 $M_\odot$	GeneratePPNtwoPN	119	9.84	0.24	0.25	0.16	102.2	Fig. 12
Baseline	NSBH	GeneratePPNtwoPN	Monotemplate	GeneratePPNtwoPN	-	9.79	0.25	0.23	0.16	100	Fig. 13
Baseline	BBH	GeneratePPNtwoPN	Monotemplate	GeneratePPNtwoPN	-	9.37	0.42	0.32	0.17	102.7	Fig. 14
Baseline	MBBH	GeneratePPNtwoPN	Monotemplate	GeneratePPNtwoPN	-	9.37	2.45	2.44	0.17	121.3	Fig. 15
Baseline	BNS	EOBNRpseudoFourPN	Monotemplate	GeneratePPNtwoPN	-	6.06	6.29	6.52	0.26	166.4	Fig. 16
Baseline	BNS	EOBNRpseudoFourPN	Grid 1.2-1.6 $M_\odot$	GeneratePPNtwoPN	73	8.56	1.49	0.88	0.19	117.9	Fig. 17
Baseline	BNS	EOBNRpseudoFourPN	Grid 1.2-1.6 $M_\odot$	EOBNRpseudoFourPN	96	9.82	0.24	0.21	0.16	102.3	Fig. 18
Baseline	BNS	EOBNRpseudoFourPN	Grid 1.2-1.6 $M_\odot$	TaylorT4threePointFivePN	113	9.84	0.24	0.22	0.16	102.1	Fig. 19
Baseline	BNS	TaylorT4threePointFivePN	Grid 1.2-1.6 $M_\odot$	EOBNRpseudoFourPN	90	9.82	0.31	0.25	0.16	102.2	Fig. 20

Figure 2: Results of the software injections runs.

Sensitivity	Inspirial type	Injected Model	Research type	Templates	Ref. freq. [Hz]	SNR (Mean)	dt [ms] (RMS)	dt [ms] (gaussian fit)	dt [ms] (theory)	Distance (Mean in %)	Plot
BBH *	BNS	EOBNRpseudoFourPN	Grid 1.2-1.6 $M_\odot$	TaylorT4threePointFivePN							
Narrow band	BNS	EOBNRpseudoFourPN	Grid 1.2-1.6 $M_\odot$	TaylorT4threePointFivePN	55	9.28	1.68	1.09	0.10	101.8	Fig. 21
Wide band	BNS	EOBNRpseudoFourPN	Grid 1.2-1.6 $M_\odot$	TaylorT4threePointFivePN	92	9.88	0.33	0.26	0.10	102.8	Fig. 22
Baseline	NSBH	EOBNRpseudoFourPN	Monotemplate 7.6-8.0 $M_\odot$	EOBNRpseudoFourPN	-	9.39	0.37	0.28	0.17	102.8	Fig. 23
Baseline	NSBH	EOBNRpseudoFourPN	Grid 1.2-1.6, 7.6-8.0 $M_\odot$	TaylorT4threePointFivePN	76	9.37	0.89	0.36	0.17	102.4	Fig. 24
Baseline	NSBH	TaylorT4threePointFivePN	Grid 1.2-1.6, 7.6-8.0 $M_\odot$	EOBNRpseudoFourPN	94	9.53	1.42	0.71	0.17	100.5	Fig. 25
Baseline	NSBH	TaylorT4threePointFivePN	Monotemplate 7.6-8.0 $M_\odot$	TaylorT4threePointFivePN	-	9.52	0.26	0.26	0.17	101.5	Fig. 26
Baseline	BNS	SpinTaylorT4threePointFivePN (Spin: 0.0-0.2)	Grid 1.2-1.6 $M_\odot$	GeneratePPNtwoPN	150	8.73	4.23	5.11	0.18	115.8	Fig. 27
Baseline	BNS	SpinTaylorT4threePointFivePN (Spin: 0.0-0.2)	Grid 1.2-1.6 $M_\odot$	EOBNRpseudoFourPN	150	9.68	3.06	1.92	0.16	103.9	Fig. 28
Baseline	BNS	SpinTaylorT4threePointFivePN (Spin: 0.0-0.2)	Grid 1.2-1.6 $M_\odot$	TaylorT4threePointFivePN	150	9.66	3.21	1.86	0.17	104.3	Fig. 29

Figure 3: Results of the software injections runs. * No injection found by Mbta.

Several different runs of software injections were made, depending on five parameters:

- the mass of the cbc (BNS, NSBH, BBH or MBBH);
- the sensitivity curve (see Fig. 1);
- the model used to generate the injections;
- the model used to generate the templates;
- the type of search used: monotemplate or with a grid of templates.

When a grid of template was used for the analysis, it was not the end time which was used to determine the timing precision of the detector, but the end time corrected to the reference frequency [7]. The following plot (Fig. 4) show how important it is to correctly chose the reference frequency used for the analysis. Indeed, when

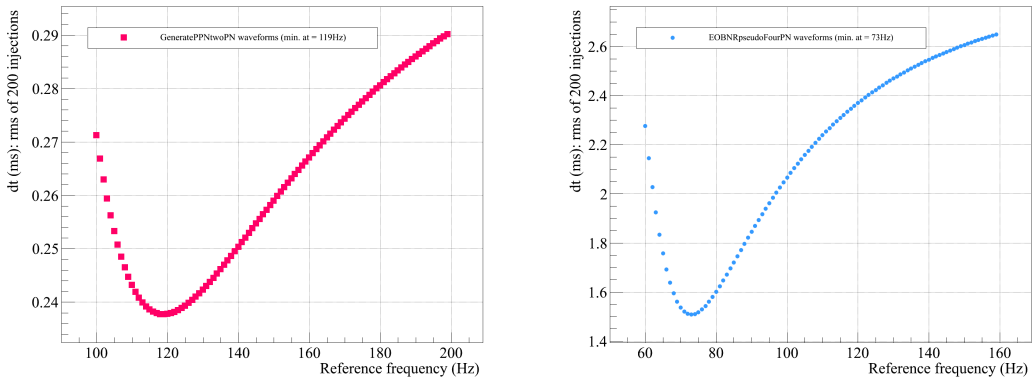

Figure 4: These plots show the timing resolution as a function of the reference frequency (AdV baseline spectrum) for two different family of injected waveforms: GeneratePPNtwoPN in the left plot, EOBNRpseudoFourPN in the right plot. In both plots, the injections were searched with GeneratePPNtwoPN templates.

looking for GeneratePPNtwoPN injections with GeneratePPNtwoPN templates, taking 150 Hz as the reference frequency instead of the optimal one (119Hz) would only imply an increase of ~ 0.01ms of the timing precision. Doing the same with EOBNRpseudoFourPN injections would imply an increase of ~ 1ms of the timing precision (150Hz instead of 73Hz). It is therefore very important to choose correctly the reference frequency used for the analysis, and all results presented in this section were obtained with the optimal reference frequency.

With this remark in mind, we may now briefly discuss the results summerized in tables 2 and 3. The first thing which comes up when looking to those tables is that, when analysing data containing one family of injections with another family of templates, using a grid of template is mandatory in order to compensate the differences between these two families of waveforms.

Let-us focus now on BNS injections. It happers that trying to detect EOBNRpseudoFourPN or TaylorT4threePointFivePN injections with GeneratePPNtwoPN templates (and vise-versa) gives very bad results. This comes from the fact that the last ones are 2PPN waveforms, while the EOBNRpseudoFourPN and TaylorT4threePointFivePN ones are higher-order waveforms. On the contrary, trying to detect EOBNRpseudoFourPN/TaylorT4threePointFivePN injections with EOBNRpseudoFourPN/TaylorT4threePointFivePN templates gives results comparable to those obtained when trying the detect GeneratePPNtwoPN injections with GeneratePPNtwoPN templates.

Things are quite differents for more massive systems. Indeed, for NSBH systems, trying to detect EOBNRpseudoFourPN injections with TaylorT4threePointFivePN templates (and vise-versa) gives less good results than those obtained when trying the detect NSBH injections with the same familiy of templates.

Finally, for BNS systems with spin (between 0 and 0.2), all three families of waveforms give very bad results. To conclude, let us stress however that these bad results may be improved by considering the time of flight between two detectors instead of the end time. Indeed, for the sake of the argument, let us consider two detecors located at the same place with two different spectrum. The time of flight (which should be zero) is ten given by (Fig. 30)

Templates	**dt [ms]**
GeneratePPNtwoPN	2.18
EOBNRpseudoFourPN	0.90
TaylorT4threePointFivePN	0.88

These last results seems to imply that the time of flight between two real detectors should not be as badly determined by Mbta for BNS systems with spin contrarily to the end time.

References

[1] F. Beauville *et al.*, Classical and Quantum Gravity **25**, 045001 (2008), [arXiv:gr-qc/0701027].

[2] The Virgo Collaboration, (2011), [arXiv 1112.6005].

[3] The Virgo Collaboration, Technical note **VIR-027A-09** (2009).

[4] S. Fairhurst, New J.Phys. **11**, 123006 (2009), [arXiv:0908.2356].

[5] M. Maggiore, *Gravitational waves: Theory and experiments (Vol1)* (Oxford University Press, 2008).

[6] LALSuite, [https://www.lsc-group.phys.uwm.edu/daswg/projects/lalsuite.html].

[7] F. Acernese *et al.*, Classical and Quantum Gravity **24**, 617 (2007).

Appendix: plots

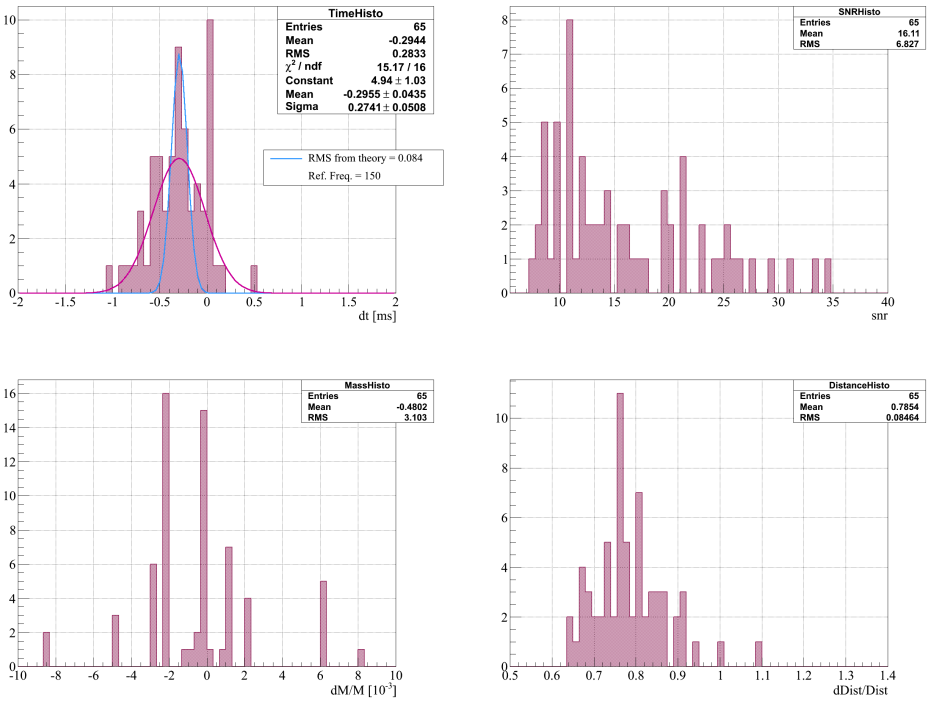

Figure 5: Hardware injection during the S6/VSR3 run: GeneratePPNtwoPN templates

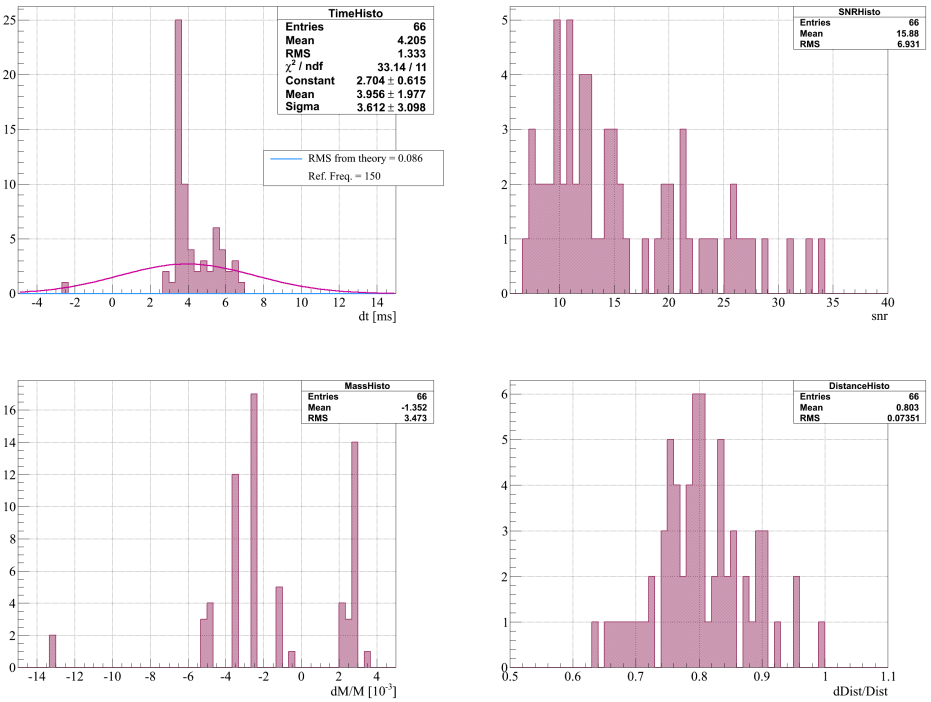

Figure 6: Hardware injection during the S6/VSR3 run: EOBNRpseudoFourPN templates

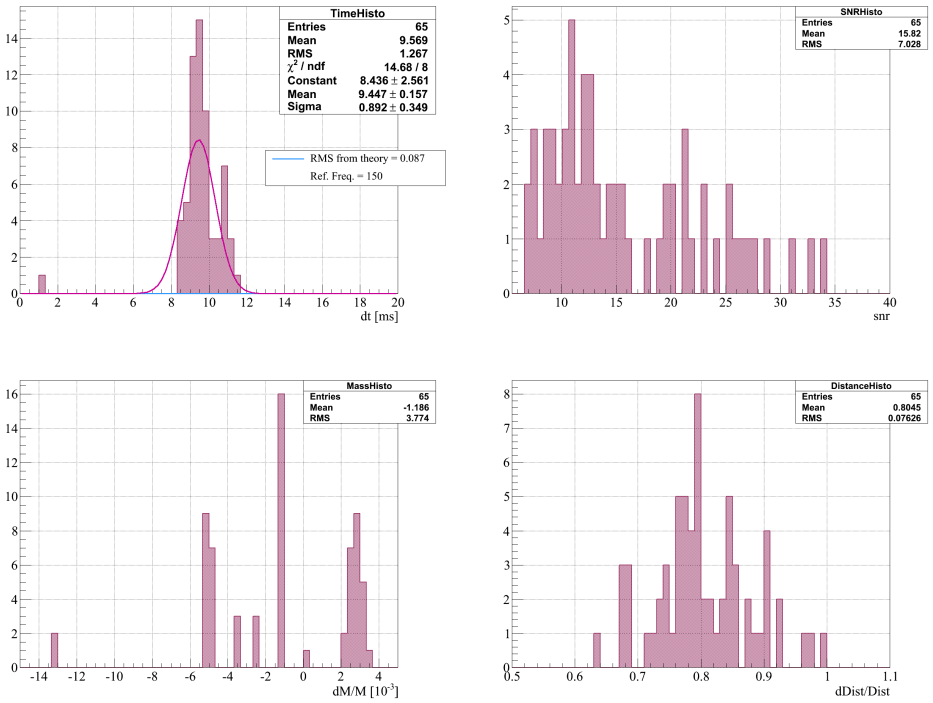

Figure 7: Hardware injection during the S6/VSR3 run: TaylorT4threePointFivePN templates

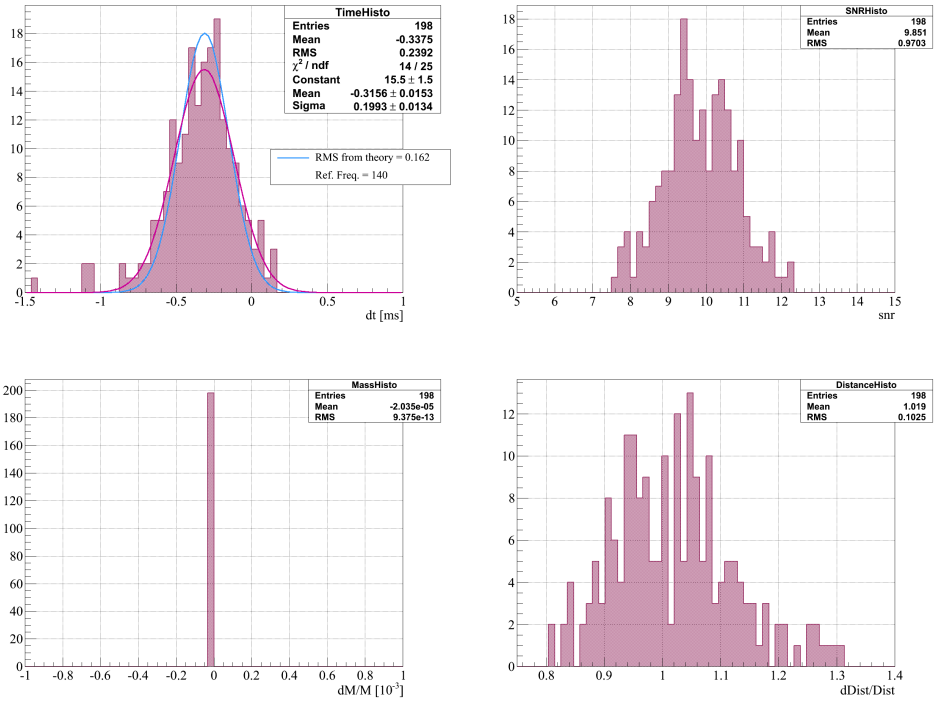

Figure 8: BNS GeneratePPNtwoPN injections, baseline spectrum, monotemplate analysis, templates GeneratePPNtwoPN

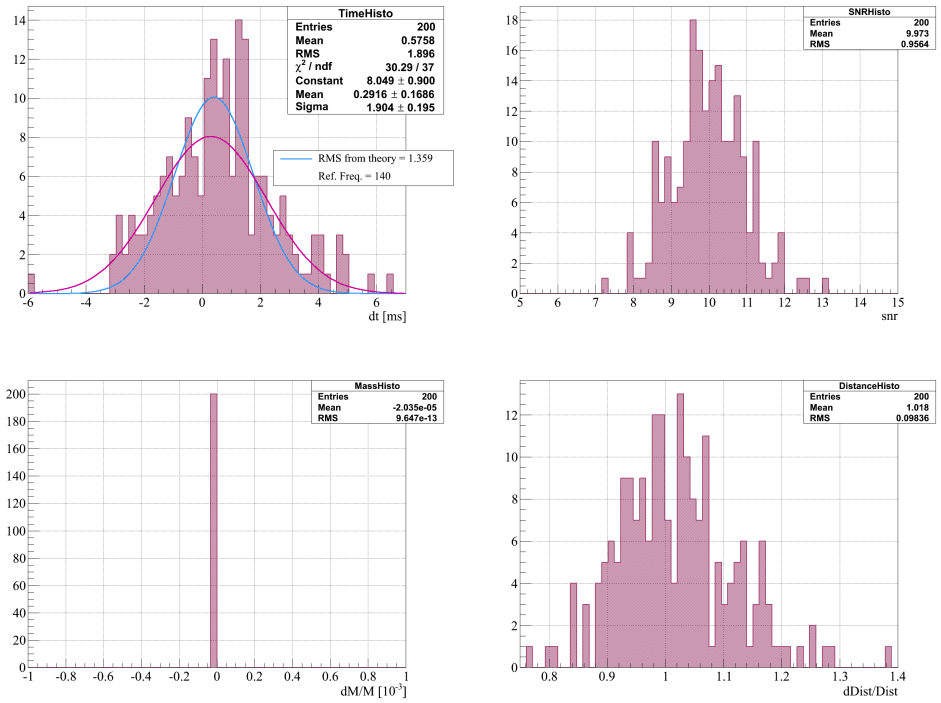

Figure 9: BNS GeneratePPNtwoPN injections, BBH optimized spectrum, monotemplate analysis, templates GeneratePPNtwoPN

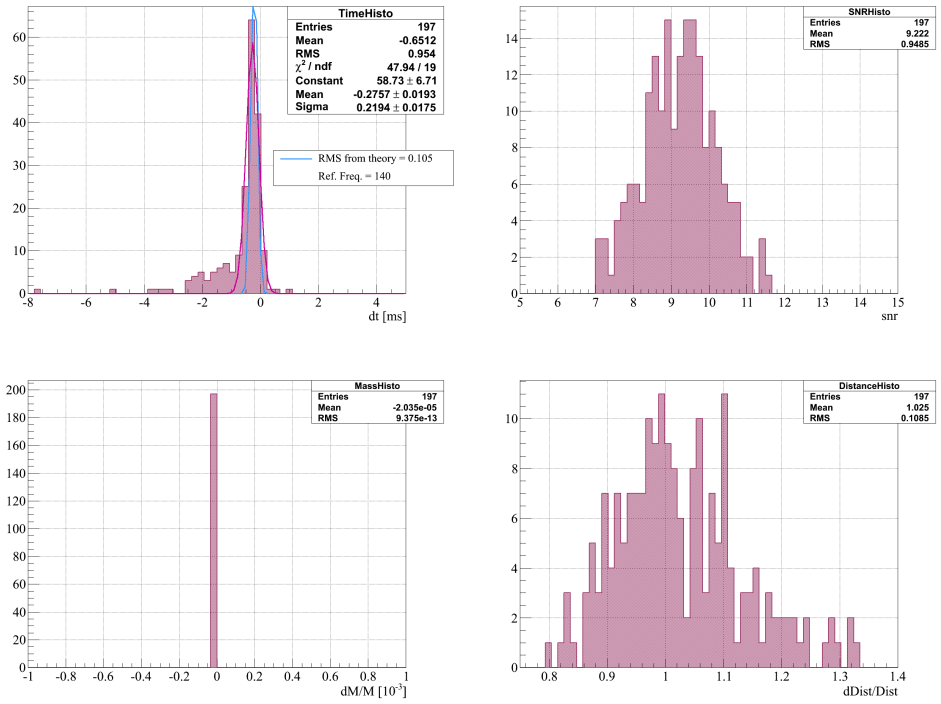

Figure 10: BNS GeneratePPNtwoPN injections, narrowband spectrum, monotemplate analysis, templates GeneratePPNtwoPN

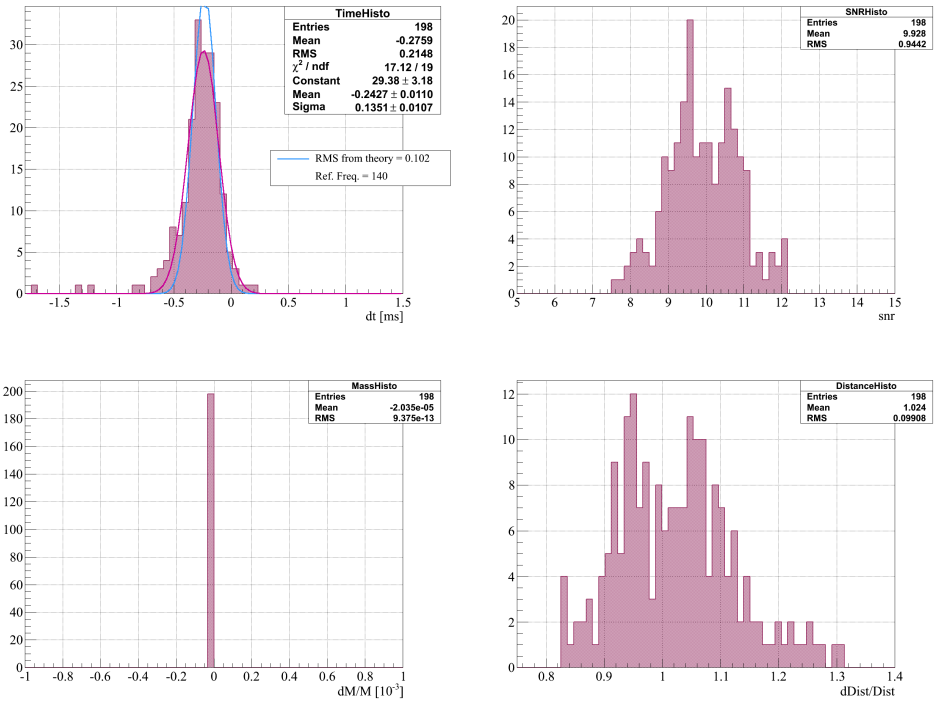

Figure 11: BNS GeneratePPNtwoPN injections, wideband spectrum, monotemplate analysis, templates GeneratePPNtwoPN

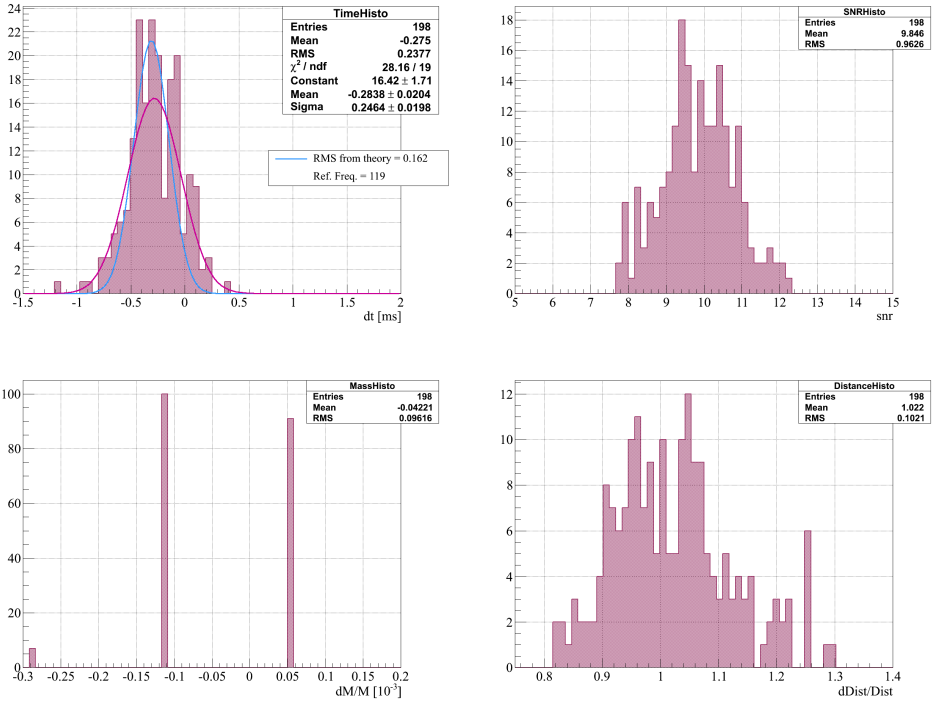

Figure 12: BNS GeneratePPNtwoPN injections, baseline spectrum, grid 1.2-1.6$M_{\odot}$, templates GeneratePPNtwoPN

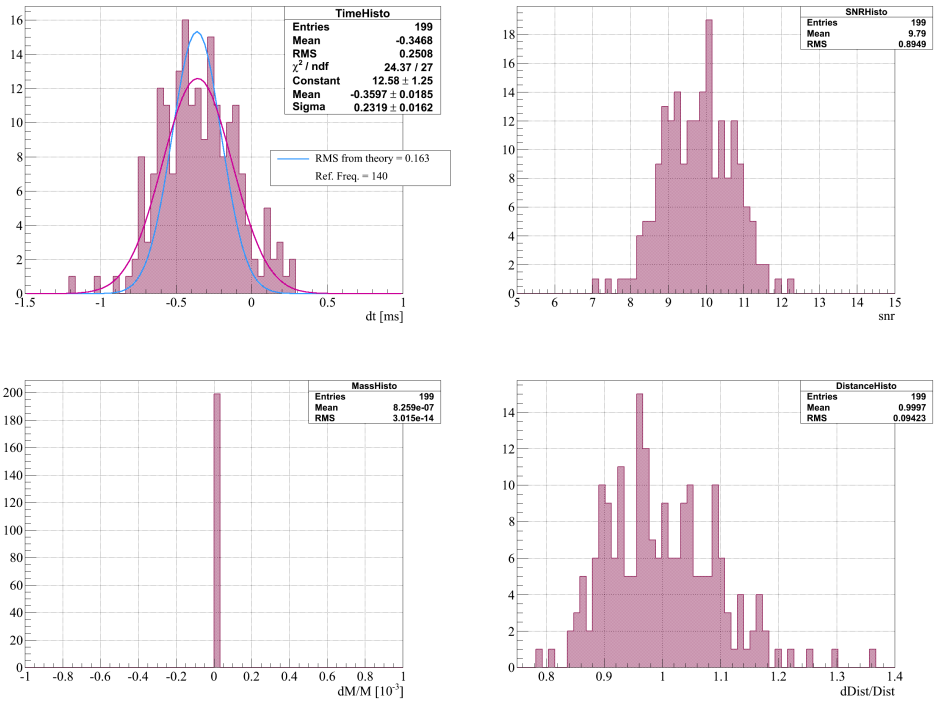

Figure 13: NSBH GeneratePPNtwoPN injections, baseline spectrum, monotemplate analysis, templates GeneratePPNtwoPN

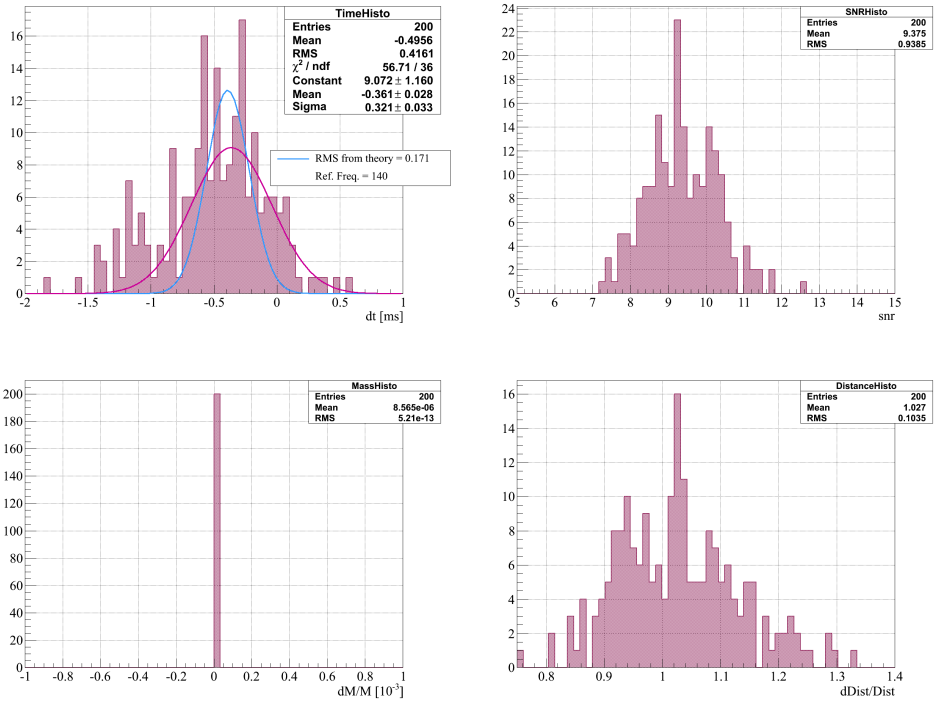

Figure 14: BHH GeneratePPNtwoPN injections, baseline spectrum, monotemplate analysis, templates GeneratePPNtwoPN

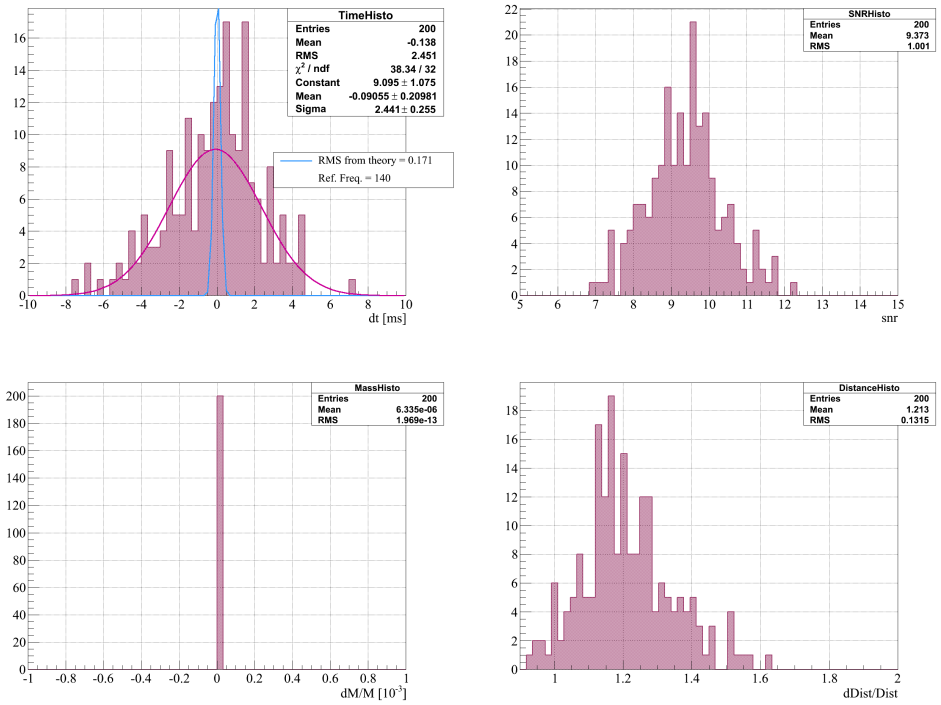

Figure 15: MBBH GeneratePPNtwoPN injections, baseline spectrum, monotemplate analysis, templates GeneratePPNtwoPN

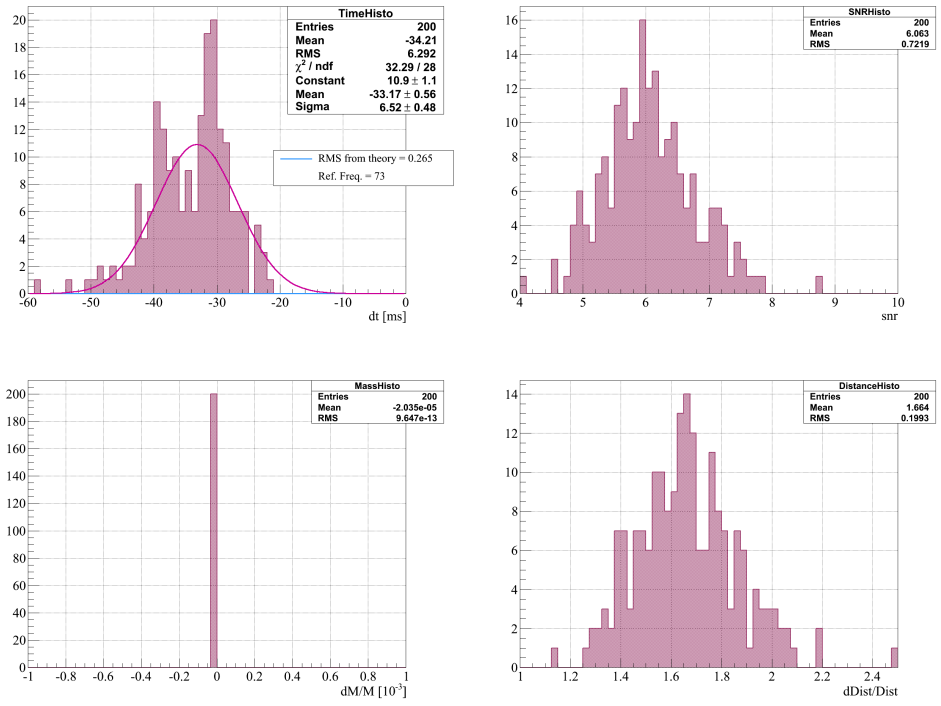

Figure 16: BNS EOBNRpseudoFourPN injections, baseline spectrum, monotemplate analysis, templates GeneratePPNtwoPN

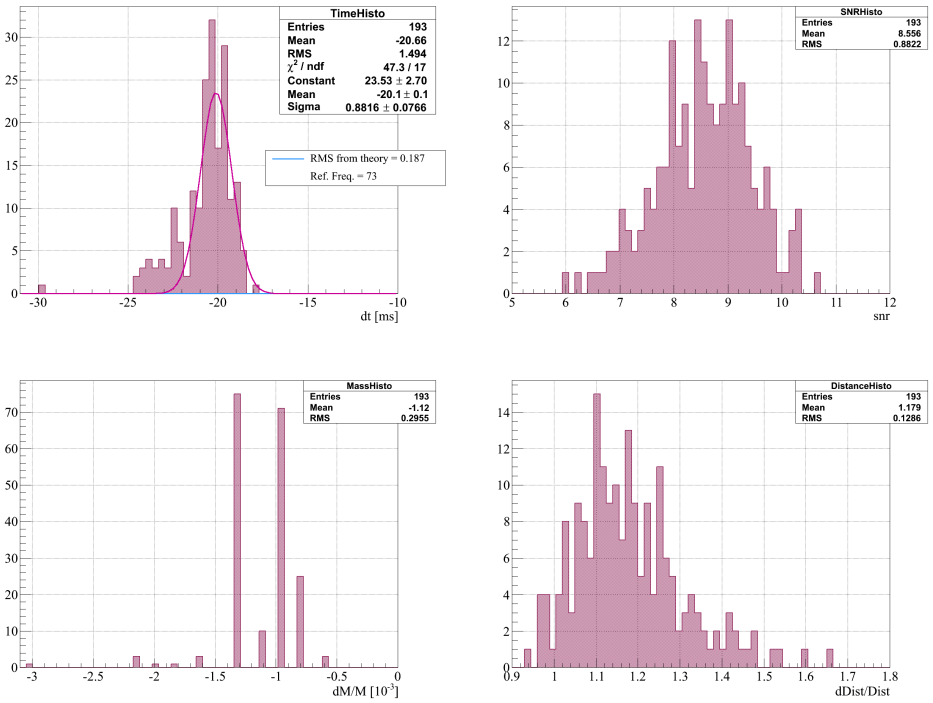

Figure 17: BNS EOBNRpseudoFourPN injections, baseline spectrum, grid 1.2-1.6$M_\odot$, templates GeneratePPNtwoPN

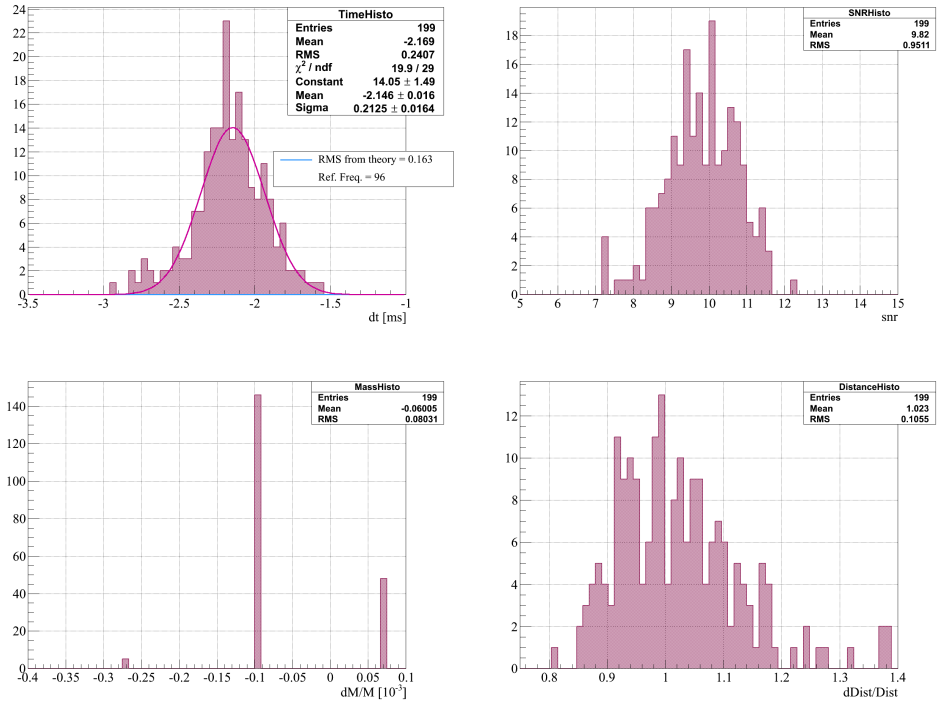

Figure 18: BNS EOBNRpseudoFourPN injections, baseline spectrum, grid 1.2-1.6$M_\odot$, templates EOBNRpseudoFourPN

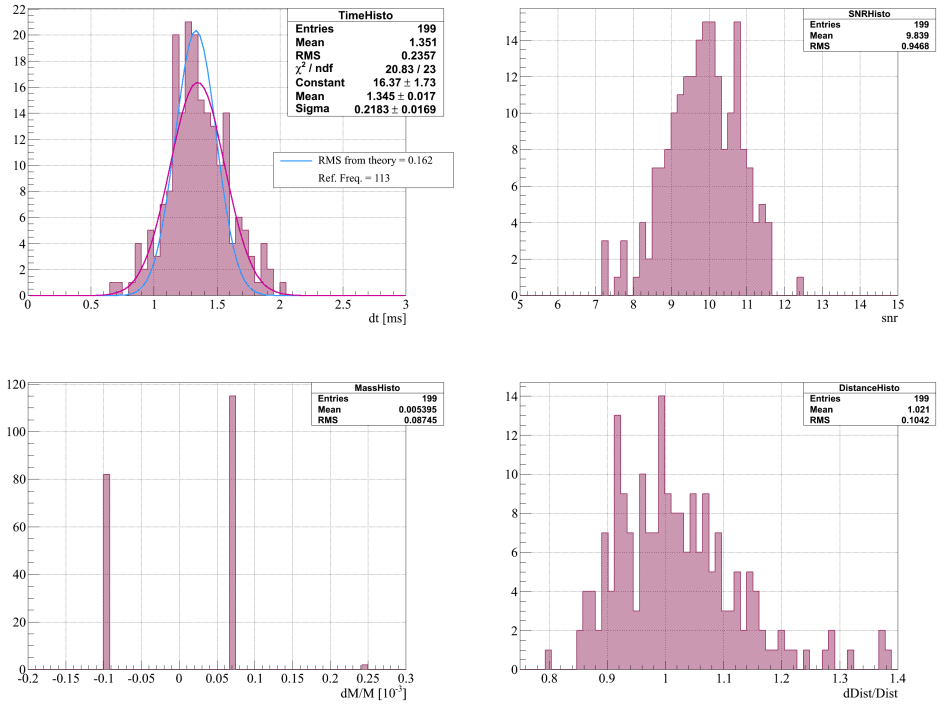

Figure 19: BNS EOBNRpseudoFourPN injections, baseline spectrum, grid 1.2-1.6$M_\odot$, templates TaylorT4threePointFivePN

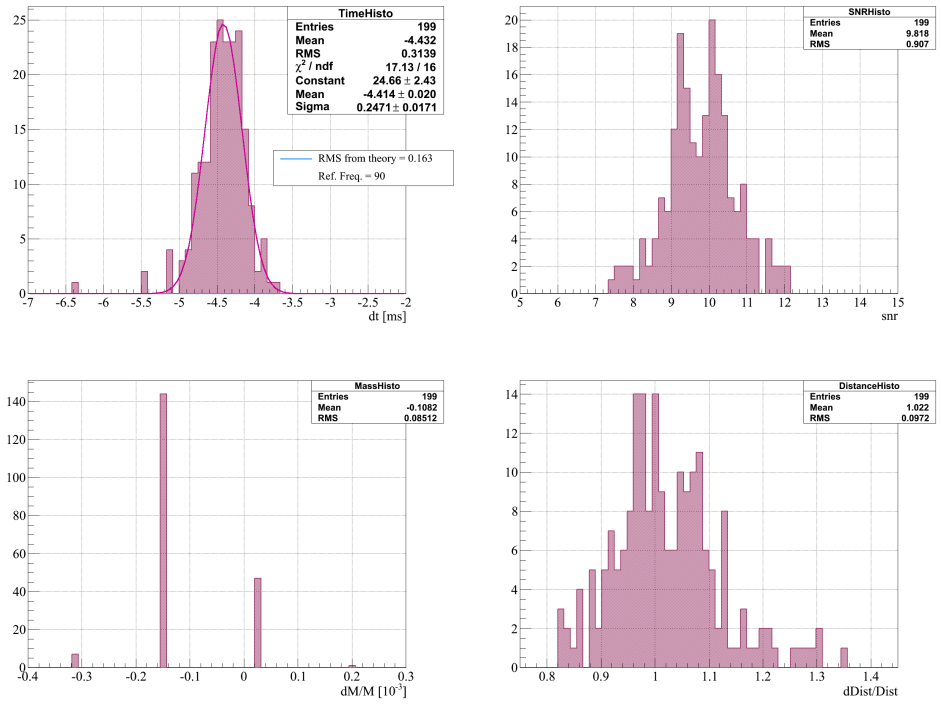

Figure 20: BNS TaylorT4threePointFivePN injections, baseline spectrum, grid 1.2-1.6$M_\odot$, templates EOBNRpseudoFourPN

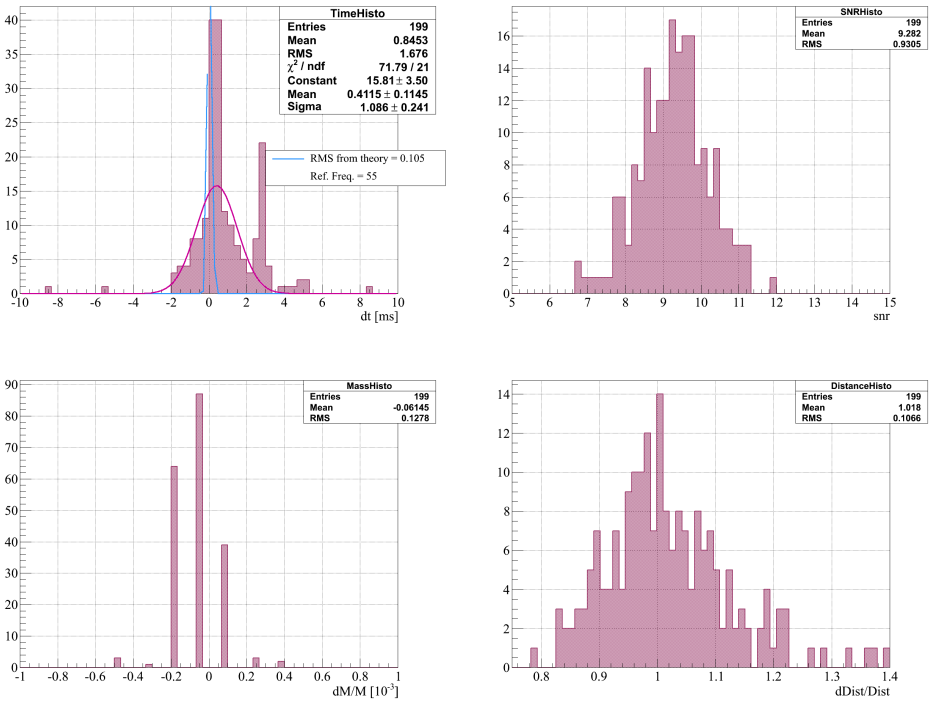

Figure 21: BNS EOBNRpseudoFourPN injections, narrow band spectrum, grid 1.2-1.6$M_{\odot}$, templates EOBNRpseudoFourPN

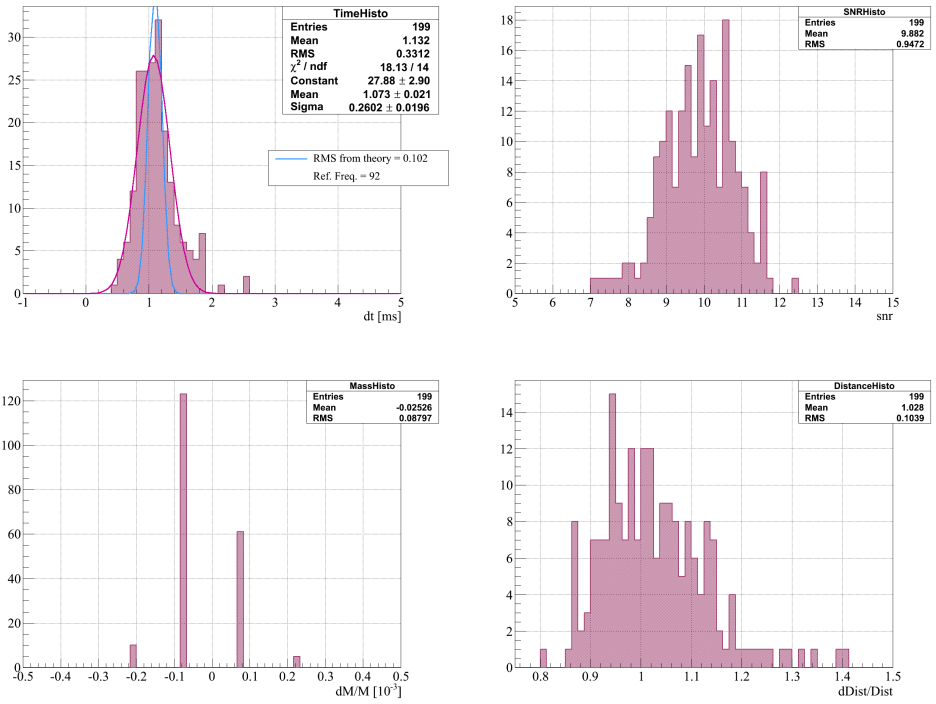

Figure 22: BNS EOBNRpseudoFourPN injections, wide band spectrum, grid 1.2-1.6$M_{\odot}$, templates TaylorT4threePointFivePN

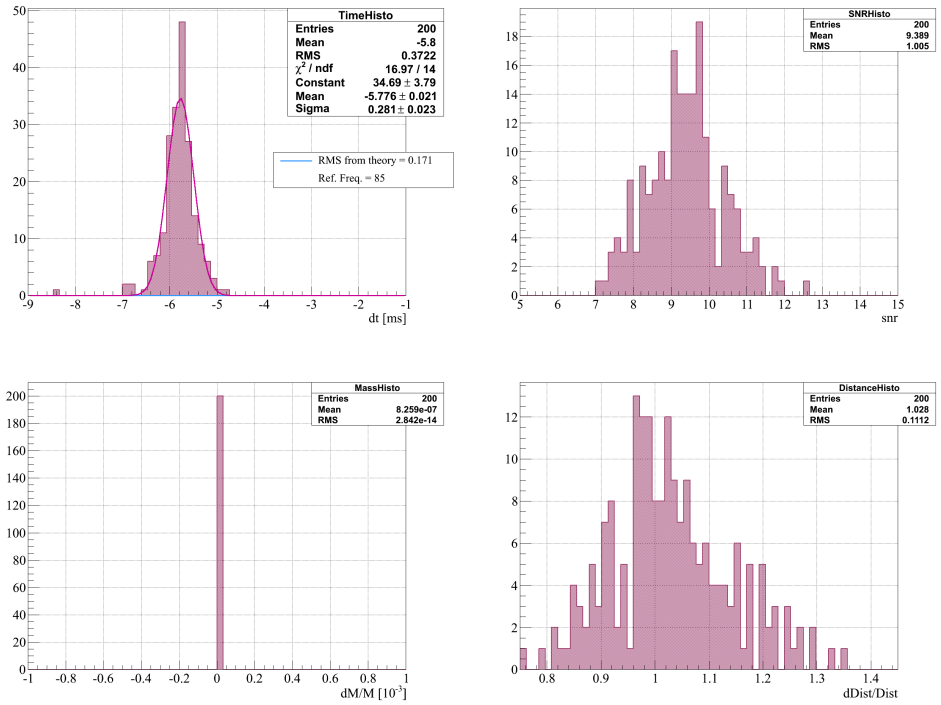

Figure 23: NSBH EOBNRpseudoFourPN injections, baseline spectrum, monotemplate analysis, templates EOBNRpseudoFourPN

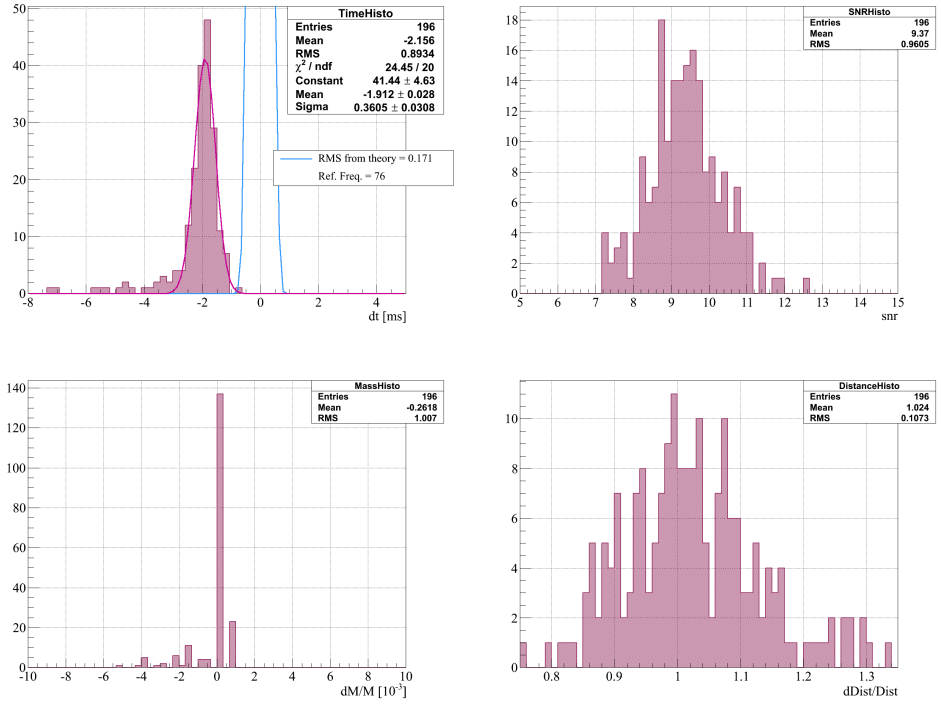

Figure 24: NSBH EOBNRpseudoFourPN injections, baseline spectrum, grid 1.2-1.6 7.6-8.0$M_\odot$, templates TaylorT4threePointFivePN

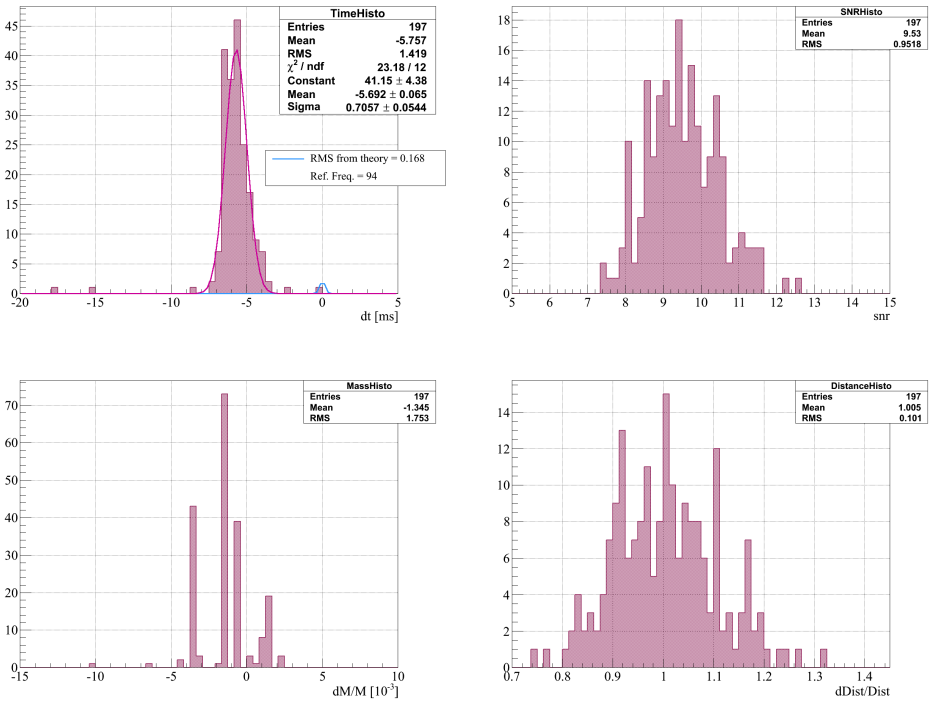

Figure 25: NSBH TaylorT4threePointFivePN injections, baseline spectrum, grid 1.2-1.6 7.6-8.0$M_{\odot}$, templates EOBNRpseudoFourPN

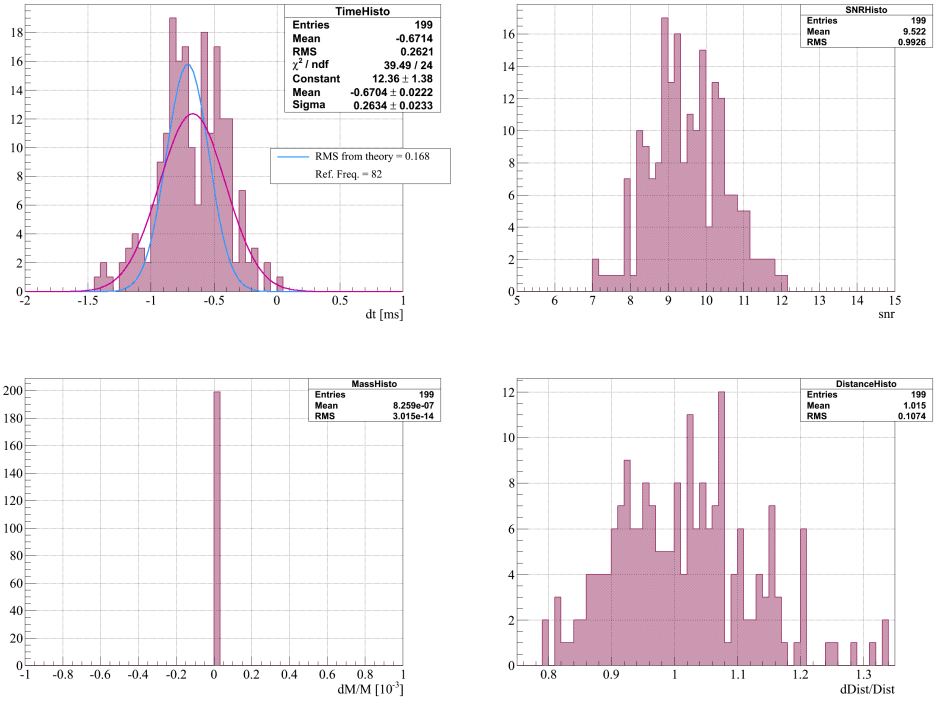

Figure 26: NSBH TaylorT4threePointFivePN injections, baseline spectrum, monotemplate analysis, templates TaylorT4threePointFivePN

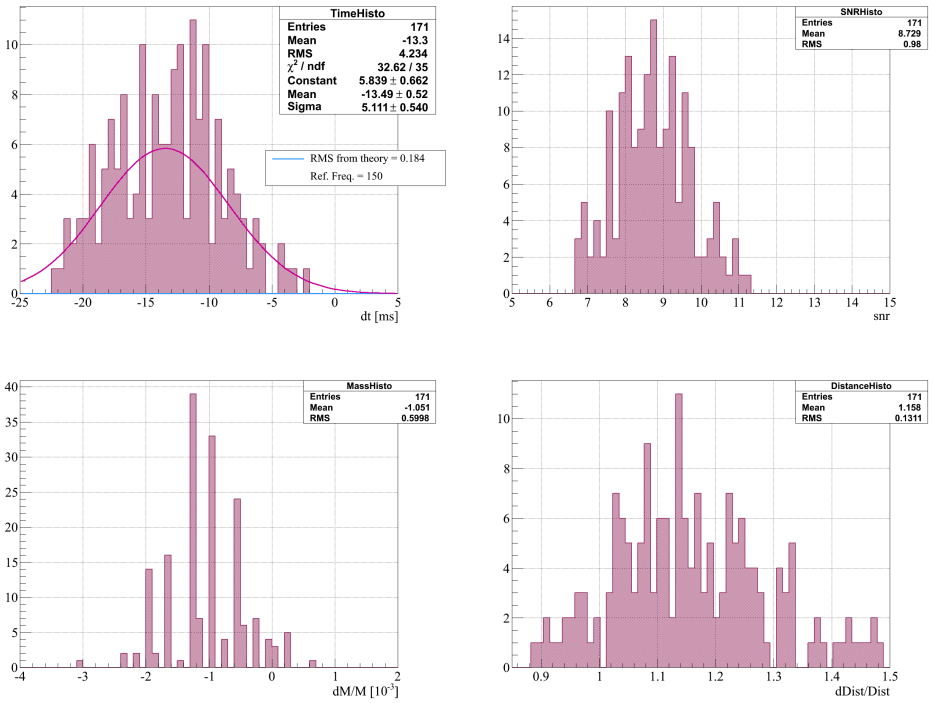

Figure 27: BNS SpinTaylorT4threePointFivePN injections (Spin: 0.0-0.2), baseline spectrum, grid 1.2-1.6$M_{\odot}$, templates GeneratePPNtwoPN

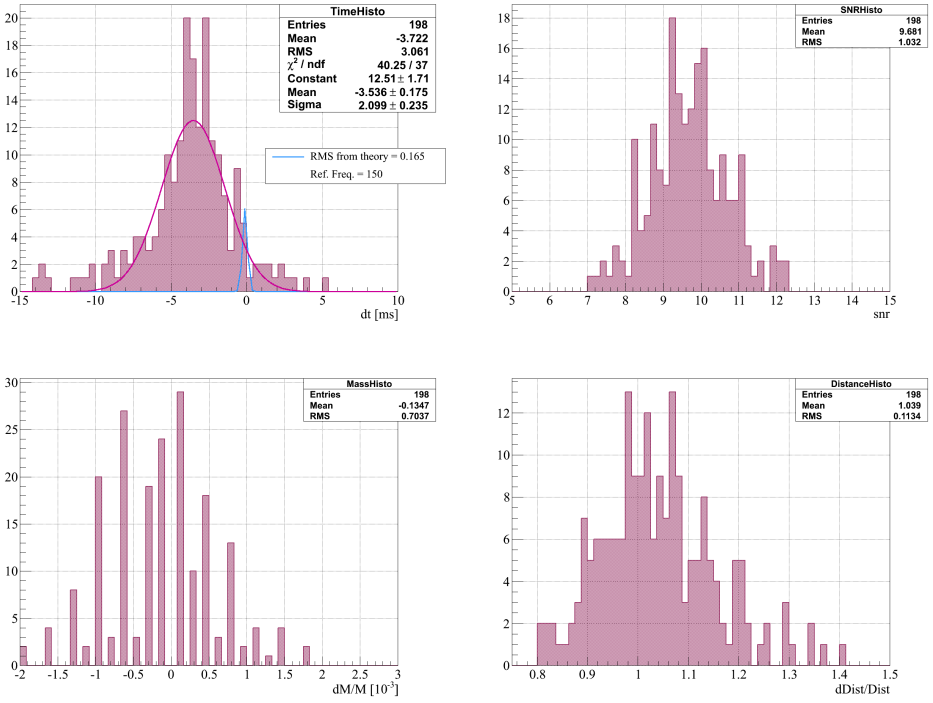

Figure 28: BNS SpinTaylorT4threePointFivePN injections (Spin: 0.0-0.2), baseline spectrum, grid 1.2-1.6$M_{\odot}$, templates EOBNRpseudoFourPN

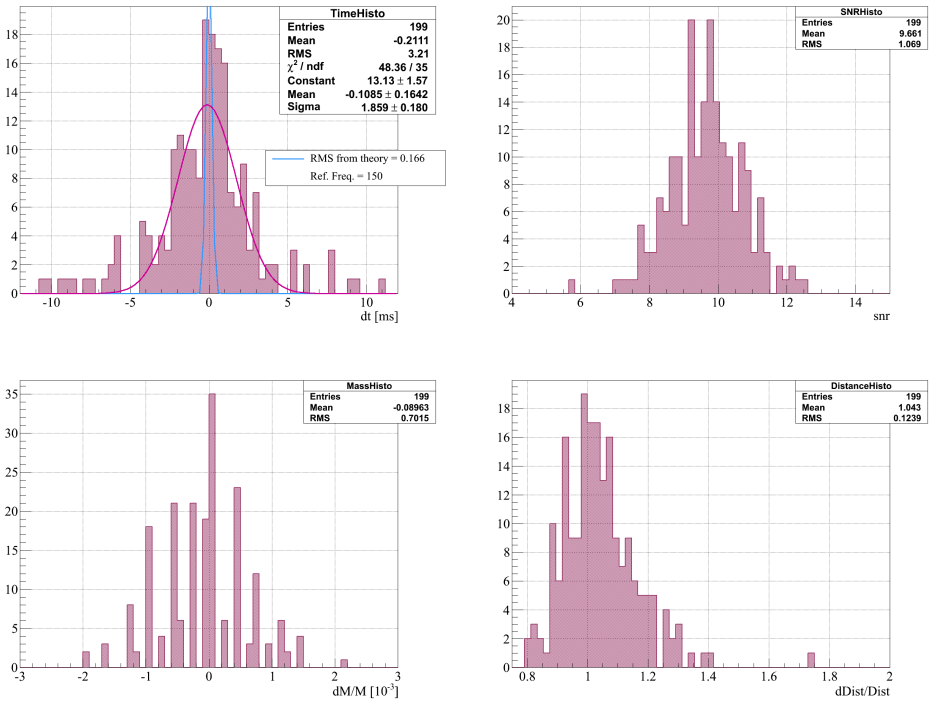

Figure 29: BNS SpinTaylorT4threePointFivePN injections (Spin: 0.0-0.2), baseline spectrum, grid 1.2-1.6$M_{\odot}$, templates TaylorT4threePointFivePN

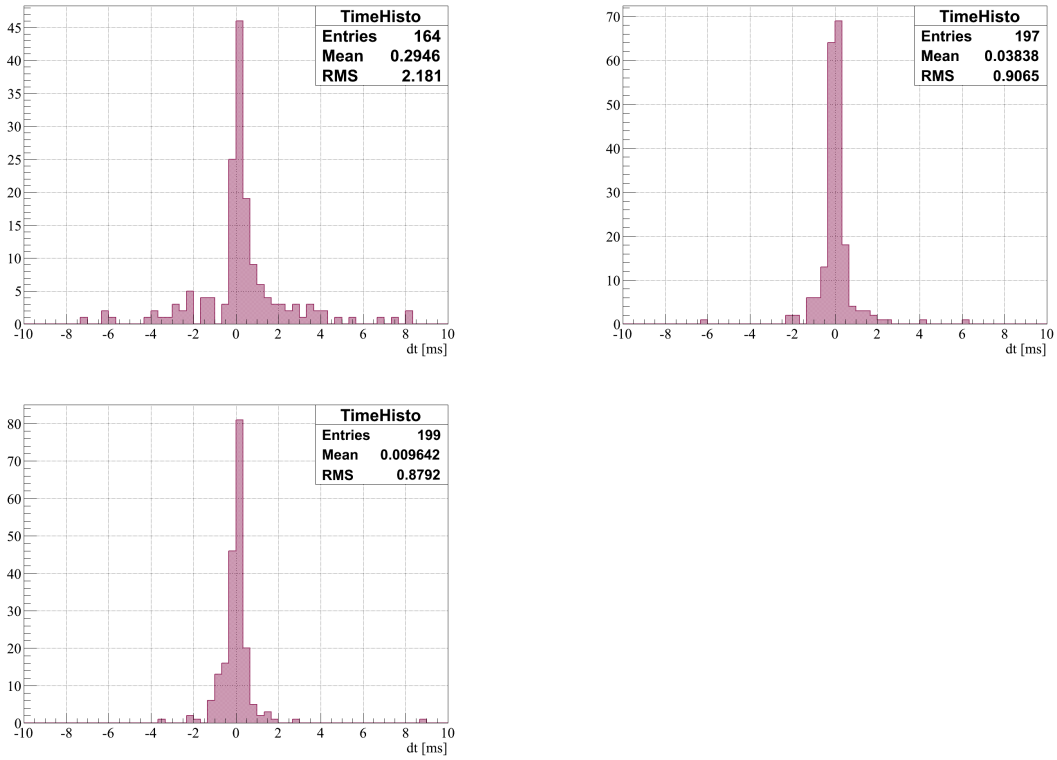

Figure 30: Time of flight for BNS SpinTaylorT4threePointFivePN injections (Spin: 0.0-0.2): two detectors at the same location, one with baseline spectrum and the second one with wideband spectrum. Grid 1.2-1.6$M_{\odot}$, GeneratePPNtwoPN templates for the first plot, EOBNRpseudoFourPN templates for the second one and TaylorT4threePointFivePN templates for the last one